

## Supernovae and High Density Nuclear Matter

S. Kahana  
Physics Department  
Brookhaven National Laboratory  
Upton, NY 11973, U S A

BNL--38289

DE86 013914

## ABSTRACT

The role of the nuclear equation of state (EOS) in producing prompt supernova explosions is examined. Results of calculations of Baron, Cooperstein, and Kahana incorporating general relativity and a new high density EOS are presented, and the relevance of these calculations to laboratory experiments with heavy ions considered.

Invited talk at International Symposium on  
WEAK AND ELECTROMAGNETIC INTERACTIONS IN NUCLEI  
Max Planck Institute for Nuclear Physics,  
University of Heidelberg; FRG  
July 1-5, 1986

**MASTER**

The submitted manuscript has been authored under contract DE-AC02-76CH00016 with the U.S. Department of Energy. Accordingly, the U.S. Government retains a nonexclusive, royalty-free license to publish or reproduce the published form of this contribution, or allow others to do so, for U.S. Government purposes.

## Supernovae and High Density Nuclear Matter

S. Kahana<sup>1</sup>  
 Physics Department  
 Brookhaven National Laboratory  
 Upton, NY 11973, U S A

## ABSTRACT

The role of the nuclear equation of state (EOS) in producing prompt supernova explosions is examined. Results of calculations of Baron, Cooperstein, and Kahana incorporating general relativity and a new high density EOS are presented, and the relevance of these calculations to laboratory experiments with heavy ions considered.

## I. INTRODUCTION

It has been known for a considerable time that the properties of nuclear matter play a significant part in stellar evolution. If the density of normal, saturated, nuclear matter,  $\rho_0 \approx 2.6 \times 10^{14} \text{ g/cm}^3$ , is taken as a standard, then for most of a star's life one needs only consider nuclear material at quite low density. During the gravitational collapse of the cores of many massive stars, however, densities several times greater than  $\rho_0$  are achieved. It is such highly compressed matter and its properties that particularly concern me here. The progenitors of type II supernovae, i.e. those supernovae whose spectra contain hydrogen lines, are believed to possess initial total mass in excess of nine or ten solar masses. I will discuss hydrodynamic simulations of collapse, carried out by Edward Baron, Jerry Cooperstein and myself [1], which are the first to produce a prompt shock-explosive mechanism for type IIs, beginning with the  $12M_\odot$  and  $15M_\odot$  models of Weaver and Woosley [2].

Over the years, two major classes of mechanism have been proposed. One approach seeks an ejection of the stellar mantle and envelope by an explosive shock created in a core bounce after collapse. A second approach would have the exterior regions blown off by the energetic neutrinos produced somewhat after collapse. Both of these scenarios are present in the classic papers of BURBIDGE, BURBIDGE, FOWLER, and BOYLE [3], and in the intervening years early work by COLGATE and collaborators [4] was carried out along both lines. Most recently, several authors (MAZUREK, COOPERSTEIN, KAHANA [5]; WILSON [6], ARNETT [7]; HILLEBRANDT [8]) have examined the collapse and subsequent shock formation with apparently negative results. Artificial initial models (COOPERSTEIN [9]; COOPERSTEIN, BETHE, and BROWN [10]; KAHANA, BARON, and COOPERSTEIN [11]) for the degenerate iron core can lead to explosions, but attempts to begin with the realistic evolutionary models of Weaver and Woosley and collaborators (WWZ [12]; WWP [13]; WW [2]) have uniformly ended with stalled, accreting shocks.

Initial quiet evolution in the more massive stars, taking some 10-100 million years, ends with a core consisting only of elements near iron in atomic number, supported by degenerate electron pressure. Collapse is first triggered by photodisintegration of iron, then by the pressure drop following rapid  $\beta$ -capture, and finally halted by the stiffening of nuclear matter at high density. Bounce occurs when densities at the outer edge of the homologously collapsing part of the core reach nuclear saturation values. A shock is inevitably formed, at or near the radius where infall and sound velocities match, i.e. at the sonic point (see Fig. 4). In question then is the outward propagation of this shock through the remaining dense material in the core, while additional material continues to rain in.

The eventual fate of the shock is determined by the initial shock energy and by the losses suffered along its path. The initial energy in the shock is clearly borrowed from the gravitational well, and the losses result from dissociation of nuclei and from neutrino escape. Interestingly, although the collapsing core mass

<sup>1</sup>The submitted manuscript has been authored under contract DE-AC02-76CH00016 with the U.S. Department of Energy.

is almost all non-relativistic nuclei or nuclear matter, it is supported by the pressure of a highly relativistic, degenerate, gas. The adiabatic index  $C_p/C_v$  for such a system is  $\Gamma = 4/3$ , and the non-relativistic virial theorem tells us that the total core energy starts close to zero. The entropy is initially low and remains low throughout collapse (BETHE and collaborators [14]); thus the process is essentially adiabatic, and the total energy stays close to zero throughout. At maximum compression, this zero core energy is divided between approximately  $100 \times 10^{51}$  ergs (100 foe<sup>1</sup>) of negative gravitational energy and  $100 \times 10^{51}$  ergs of internal energy. Since only one foe emerging in the shock is sufficient to unbind the mantle and envelope (bound by a few tenths of a foe) as well as produce the required visual display, one must be prepared to carry out an accurate calculation on a delicately balanced system.

The early work of MAZUREK, COOPERSTEIN, and KAHANA [5] began with the 10-25  $M_\odot$  models of WEAVER, WOOSLEY, and ZIMMERMAN [12] and found stalled shocks. It was argued that excessive neutrino escape and dissociation were responsible for the enfeebled shock. However, WWZ [12] models ascribed a mass of 1.51  $M_\odot$  to the initial iron core. The shock could simply not traverse so much dense material in the highly compact core. In further work by WEAVER, WOOSLEY, and FULLER (WWF) [13] the omission of important  $\beta$ -capture channels was corrected, the initial electron fraction  $Y_e$  lowered, and hence the effective core mass (recall  $M(\text{Chandrasekhar}) \sim 5.6 Y_e^2$ ) was reduced to 1.36  $M_\odot$ . We shall see that, though the WWF core is more diffuse than that of WWZ, we were still unable to successfully simulate type II supernovae. Our development (BARON, COOPERSTEIN, and KAHANA [1]) depends critically on the equation of state used for nuclear matter at high density and on the introduction of relativistic gravitation into the collapse phase. By theoretically altering the equation of state, corresponding to a softening of high density matter, we are able to increase the energy initially pumped into the shock. In a purely Newtonian calculation this change is not sufficient. Paradoxically, it is the introduction of general relativity, despite the apparent harm caused by the strengthening of gravitation, in combination with the softer matter that leads to a successful theoretical mechanism.

## II. THE EQUATION OF STATE

### Role in Supernovae Studies

Driven by the exigencies of the supernova problem, we have in earlier work employed as simple an equation of state as permitted [1,11,15]. Such an approach is justified not only from calculational necessity, i.e. reduction in computing time, but also from informational reality. Considerable theoretical knowledge and experimental constraint can be brought to bear on the nuclear equation of state at densities below the saturation value  $\rho_0(x)$ ,  $x=Z/A$ , for normal nuclear matter. At higher density, however, little is known from laboratory experiment. A second point in favour of simplicity is the restricted sensitivity of the collapse calculations to various components in the equation of state. Baldly put, the collapsing stellar core near maximum compression senses some average compressibility at saturation and some average adiabatic index over a range of densities from  $\rho_0$  to perhaps 3-4  $\rho_0$ , and little else.

Another relevant issue to keep in mind, missed by many earlier workers, is the actual environment in the stellar core at collapse. In particular, the charge to mass ratio,  $Z/A = Y_e$  drops to the value  $x = .32$  because of  $\beta$ -capture. For densities greater than  $\rho_0(Z/A)$ , equal to  $2.4 \times 10^{14}$  gm/cm<sup>3</sup> for  $Z/A = 1/3$ , we then suggested the simple form

$$P_N(\rho) = \frac{K_0(Z/A) \rho_0(Z/A)}{9\gamma} [u^\gamma - 1], \quad u = \rho/\rho_0(Z/A) \quad (1)$$

for the cold nuclear pressure. Here  $K_0$  is the nuclear modulus of incompressibility at saturation, i.e.  $u = 1$ , and at the charge to mass ratio  $Z/A$ , while  $\gamma$  is the limiting adiabatic index at high density. The corresponding nuclear energy per baryon is

$$E/A = -16.0 + 29.3 \left(1 - \frac{2Z}{A}\right)^2 + E_D + \frac{\pi^2 \tau^2}{4c_F^2} \cdot u^{-2/3} \text{ MeV} \quad (2)$$

<sup>1</sup>G. E. Brown is responsible for the unit 1 foe =  $10^{51}$  ergs.

with the cold compressional energy

$$E_p = \int_{\rho_0}^{\rho} dp \frac{P_N}{\rho^2} = \frac{K_0}{9\gamma(\gamma-1)} \left[ u^{\gamma-1} + \frac{\gamma-1}{u} - \gamma \right]. \quad (3)$$

The thermal energy in (1) is that of a non-interacting Fermi gas, incorporating correlation effects only through the effective mass in the Fermi energy  $\epsilon_{F,0} = p_F^2/2m^*(p_F)$ . Thus, our equation of state for dense nuclear matter can be viewed as containing three unknown parameters,  $K_0(Z/A)$ ,  $\gamma$ , and the effective mass. Figure 1 displays  $P_N$  from (1) as a function of density and parametrically of  $\gamma$ .

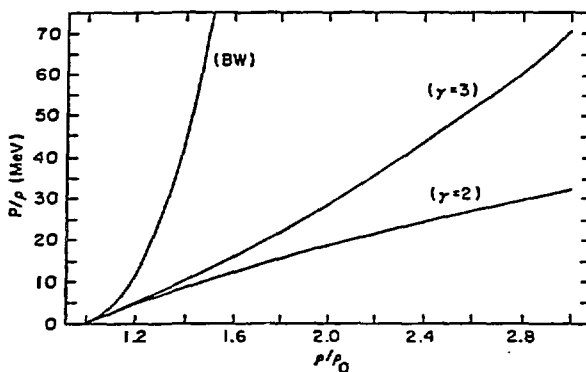


Fig. 1. Pressure versus densities are given for the Baron, Cooperstein, Kahana high density equation of state for two values of the parameter  $\gamma$  (the high density adiabatic index) in (1). For comparison, the same curve is shown for a very stiff equation of state (Brick Wall) in an artificially constructed model.

At the high densities reached in the collapsing cores of supernovae, and certainly at the perhaps even higher densities of the final compact remnant (presumably a neutron star), two forms of matter may compete for dominance: the hadronic matter I have considered and quark matter. Expressing the baryon equation of state in terms of the thermodynamic parameters, volume, chemical potential ( $\mu$ ) and temperature, and then recalling the phenomenological equation of state (at  $T=0$ )

$$P_{\text{quark}} = a' \cdot \mu^4 - B, \quad \text{with } B \text{ the bag pressure}, \quad (4)$$

allows one to get some handle on the transition point. The main point I make here is to note the ambiguities inherent in proceeding with hydrodynamical simulations based on too elaborate an equation of state and in assuming only hadrons are present, even though the transition density is not achieved during collapse. Equation (1) should then be thought of as playing a phenomenological, symbolic role.

#### Asymmetric Matter

Recall also, as I have indicated above, that in the collapse environment  $\beta$ -capture has reduced the electron fraction, i.e.  $Y_e$  to near 1/3. The incompressibility  $K_0$  is a strong function of the asymmetry of nuclear matter, a point first made in BARON, COOPERSTEIN, and KAHANA [15]. Using knowledge of the symmetry energy, BCK arrived at the simplified expressions

$$\begin{aligned} K_0(Z/A) &= K_0(1/2) [ 1 - a(Z/A - 1/2)^2 ] \\ \rho_0(Z/A) &= \rho_0(1/2) [ 1 - b(Z/A - 1/2)^2 ] \end{aligned} \quad (5)$$

which for  $a=2$ ,  $b=3/4$  yield a good representation of the calculations of KOLEHMAINEN and collaborators [16]. Since

$$\frac{K(\rho)}{9} = \left[ \frac{\partial P}{\partial \rho} \right]_{\rho_0} = \rho_0^2 \left[ \frac{\partial^2 E}{\partial \rho^2} \right]_{\rho_0}, \quad \left[ \frac{\partial E}{\partial \rho} \right]_{\rho_0} = 0, \quad (6)$$

it is clear that somewhere between  $Z/A = 1/2$  and completely asymmetric neutron matter,  $Z/A = 0$ ,  $K_0(Z/A)$  must vanish; the saturation minimum becomes a point of inflection and then disappears. Most of the softening we require, to achieve theoretical explosions, from the BLAIZOT [17] value for  $K_0(1/2)$  that I later discuss, results from the extrapolation exhibited in (5). The development in this section runs contrary to the oft-stated opinion that asymmetric matter is "stiffer" than symmetric matter. This statement is presumably based on the true but misleading changes in effective forces expected as one goes towards neutron-rich matter. The only meaningful density at which to cite a compression modulus is the saturation value  $\rho_0(Z/A)$ . Clearly from (5) this incompressibility decreases as  $Z/A \rightarrow 0$ , i.e. asymmetric matter is softer at saturation than is symmetric matter; this effect is heightened by the  $[\rho_0]^2$  factor in (6) coupled to the behaviour of  $\rho_0(Z/A)$  exhibited in (5).

#### Nuclear Compressibility Information from Low-lying Excitations

Since the changes in the properties of nuclear matter we require are somewhat controversial, I would now like to consider briefly just what information we have about  $\Gamma(\rho)$  and  $K_0(Z/A)$  (and  $m^*(p_F)$ ) at the densities achieved in the central core at bounce. We can of course get  $K_0$ ,  $\gamma$ , and  $m^*$  directly from nuclear matter calculations, but it is also interesting to bring whatever empirical evidence exists directly to bear. In terms of the Landau parameters  $F_l(l=0,1,\dots)$  characterising the effective particle-hole interaction in nuclear matter, one can write

$$\begin{aligned} K_0 &= 6\epsilon_F(1 + F_0) \\ m^*(p_F) &= m[1 + F_1/3]. \end{aligned} \quad (7)$$

In the simplified case of Skyrme forces BLAIZOT [17], whose development I follow here, derives the result

$$K_0 = \frac{a}{\rho_0} - \frac{9\epsilon(\rho_0)}{\rho_0} + d \left[ \frac{-9\epsilon(\rho_0)}{\rho_0} + \frac{3a}{\rho_0} \right] \quad (8)$$

where  $\epsilon(\rho_0)$  is the energy density functional at saturation and  $a = \frac{3\hbar^2 k_F^2}{10m} \rho_0$ ,

while the force is given by

$$v(\underline{r} \cdot \underline{r}') = 1/V(\epsilon_0 + \epsilon_3 \rho^d) \delta(\underline{r} - \underline{r}') \quad (9)$$

For the choice  $k_F = 1.35 \text{ fm}^{-1}$  and  $\epsilon(\rho_0)/\rho_0 = -16 \text{ MeV}$ , Blaizot [17] obtains  $K_0 = 167 + 212d \text{ MeV}$ .  $K_0$  then varies between 238 MeV and 96 MeV for  $d$  varying between  $1/3$  and  $-1/3$ , corresponding effectively to an increase in the range of the force. To relate these quantities in infinite matter directly to finite nuclear information, Blaizot [17] performed a random phase calculation (RPA) for the energy of the breathing mode in heavy nuclei. His results are summarized in Fig. 2.

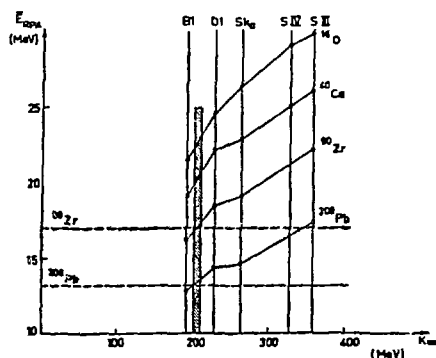


Fig. 2. The RPA predictions of Blaizot for the breathing mode in  $^{208}\text{Pb}$  and  $^{90}\text{Zr}$  compared to the experimental values (dashed lines). The vertical lines indicate the calculations for different forces used in the RPA. B1 and D1, which give results closest to experiment, are both finite range forces, while Skyrme forces  $\text{Sk}_a$ , SIV, and SIII all give larger compressibilities and disagree with experiment. The infinity in  $K_\infty$  (and  $\rho_0(\infty)$  above) refers to the infinite matter limit.

A major problem in this standard treatment of finite nuclear compressibility is apparent in the relation for  $K_0(1/2)$  in terms of  $F_0$  and  $m^*$ . The effective mass is evaluated at the Fermi surface, whereas the single particle (hole) states involved in the finite nucleus RPA are appreciably removed from  $F_F$ . The well publicized difficulty in reproducing known single particle levels above and below the closed shell nucleus  $^{208}\text{Pb}$ , with the quasi-zero range forces like Skyrme and its variants, is a strong warning in this regard. The two particle correlations in the RPA shift the monopole resonance some 14 MeV downwards, and are an added complication. I personally feel we are a long way from pinning down the incompressibility of nuclear matter at saturation; nevertheless, I feel Blaizot's result,  $K_0(1/2) = 210 \pm 30$  MeV, is an honest and useful estimate.

#### Relativistic Heavy Ion Collisions

The analyses of relativistic heavy ion experiments performed at Lawrence Berkeley Laboratory by STOCK, HARRIS, and collaborators [18,19] and GUSTAFSSON, GUTBROD and collaborators [20] are also viewed as a commentary on the nuclear EOS. Two differing phenomena: (1) pion production in heavy ion collisions, and (2) the transverse momentum distributions of collision fragments, are used to deduce information on the state of matter. The extraction of an infinite matter compressibility from such analyses is complicated in this instance by the non-equilibrium nature of the actual collision and perhaps also by the fairly high temperatures achieved.

In the case of pion production (HARRIS and collaborators [18,19]; KITAZOE and collaborators [21]) the reasoning is simple: energy generated in the nuclear medium by collision is divided into compressional and thermal components, with only the latter available for pions. One imagines a division of nuclear matter into two regions, one collision-free or unshocked, and one shocked, in which all pions are generated. Presupposing chemical equilibrium for the two baryon species N and  $\Delta$ , one obtains for the pion multiplicity

$$\langle m_\pi \rangle = \frac{\rho_\pi + \rho_\Delta}{\rho_N + \rho_\Delta} = \frac{\rho_\pi + \rho_\Delta}{\rho} \quad (10)$$

The relativistic Rankine-Hugoniot equations applied for a one-dimensional geometry are then used to derive the conditions in the shocked region 2 from the known state

of normal nuclear matter  $\rho_1 = \rho_0(1/2)$  in the unshocked region 1.

The form of the compressional energy used in the LBL analyses [18,19] is the so-called parabolic dependence

$$P_\rho = \frac{K_0 \rho_0}{9} u^2 (u - 1), \quad \Gamma(\rho) = 3 + \frac{1}{u-1}. \quad (11)$$

Eq. (11) can be compared to the BCK equation of state, i.e., to eq. (1). From (1) it appears the parabolic form, for equal  $K_0$ , generally is stiffer than BCK with  $\gamma \leq 3$ .

Baron, Brown, Cooperstein, and Prakash [22] have attempted to pursue a fundamental derivation of the high density EOS by introducing necessary relativistic effects. Figure 3 from these authors presents comparative results for  $\langle m_\pi \rangle$  from BCK and from the parabolic form. Clearly with  $K_0 = 400$  MeV, an even stiffer EOS than afforded by  $\gamma = 4$  in BCK, for which the parabolic and BCK forms are roughly equivalent, is required by the data. The stiffer the EOS employed, the less energy available for pions. A cold compressibility of  $K_0 = 600-800$  MeV seems necessary to fit the pion data [18,22].

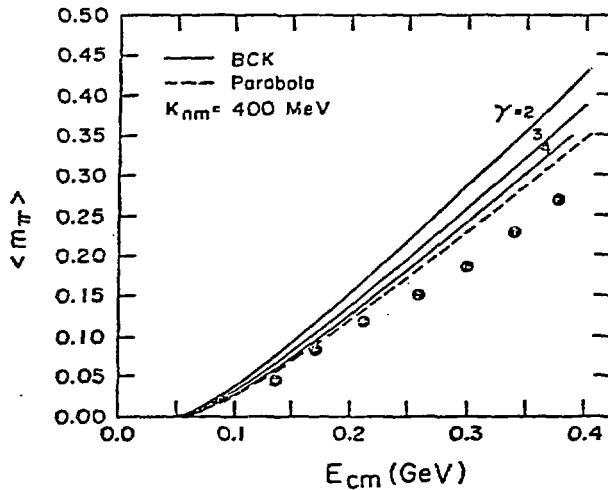


Fig. 3. Heavy-ion pion production. Comparisons of BCK for  $\gamma=2,3,4$  and of the "parabolic" EOS with the data for the number of pions/baryons,  $\langle m_\pi \rangle$ , produced in heavy ion collisions, from Baron and collaborators [22]. The data is best fitted by an even stiffer EOS with  $K_0(1/2) = K_{nm} = 600-800$  MeV.

BARON and collaborators [22] argue that the nuclear EOS is indeed stiffer at higher temperature, e.g. at the  $T = 70$  MeV reached in the experiments. Their argument exploits the weakening in the attractive tensor force occasioned by higher average excitation energies in colliding matter. Similar conclusions, but not so extreme with respect to the degree of stiffness, follow from an analysis of sideways flow in heavy ion collisions (GUSTAFSSON and collaborators [20]; MOLITORIS and STOCKER [23]).

This disagreement between compressibilities, already present between the two different analyses of nuclear properties considered, is again exhibited in the hydrodynamic evolution of stellar collapse I now turn to. Ironically, it is only in the distant stellar laboratory that truly uniform nuclear matter obtains in conditions of chemical and thermal equilibrium.

### III. HYDRODYNAMIC SIMULATION: NEWTONIAN

The hydrodynamic scheme I discuss here is based on a Newtonian code developed by Cooperstein [9] and used extensively in earlier work with my collaborators [11,15]. The force equation being studied for a spherically symmetric distribution of matter with velocity field  $U(r,t)$  is

$$\rho \frac{dU}{dt}(r,t) = -G \frac{\rho(r) m(r)}{r^2} - \frac{dP}{dr}, \quad \text{with } P = P_N + P_{\text{lept}}. \quad (12)$$

The mass  $m(r)$  within the sphere radius  $r$  provides a Lagrangian coordinate for the problem. Supplementing (12) one must have some treatment of the only non-equilibrium aspect of this problem, neutrino transport. Wilson [6] has included a more complete diffusion approach in his calculations, and these provide a normalizing standard. In BCK [1,11,15] two approximate treatments are employed: (1) trapping at some density plus free-streaming, or 2) leakage (EPSTEIN and PETHICK [24]). The leakage scheme permits neutrinos to escape from all zones in the star, and was conservatively designed to over estimate the escape. Energy is explicitly conserved in all these Lagrangian schemes.

The Newtonian simulations performed following the early work of MAZUREK, COOPERSTEIN, and KAHANA [5] were intended for answering one question: What is the sensitivity of shock stalling to the nuclear EOS above (and just below) saturation density? We recognized early on that little constraint is provided here by laboratory experiment, and also we felt that the shock energy would be clearly enhanced by a softening of the high density matter. Increased gravitational compression of the "spring" in the stiffening matter would leave the final hydrostatic core more bound, and could result in the increased transfer of energy to the shock. The realistic initial models used were those of WEAVER, WOOSLEY, and FULLER [13] with central entropies of 0.67 per baryon (in units of  $k_B$ ) and with a core mass of approximately  $1.36 M_{\odot}$ , much to be preferred to the  $1.51 M_{\odot}$  core of WWZ [12].

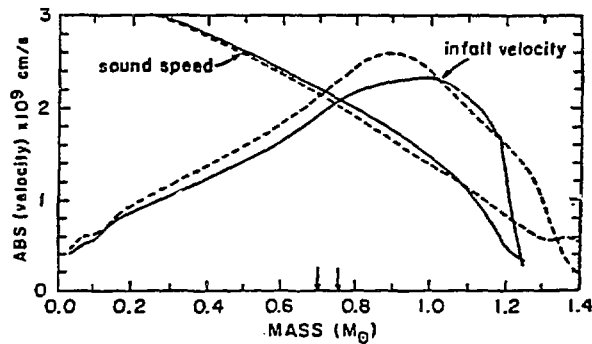


Fig. 4. The sonic point is displayed for two artificially constructed Newtonian models, FAIL and EXT. The dotted lines refer to the model FAIL, which produced a stalled shock, and the solid lines refer to model EXT (TREME), which ended in a successful explosive shock. Note the small mass difference between the formation of the sonic point in the two models (indicated by the arrows on the abscissa). This small mass difference is quite important to the shock propagation.

Other, artificially generated, models were examined to study the effects of a softer EOS and also to study shock energy loss during outward propagation. Table I, reproduced from BCK [15], illustrates the role of the EOS, while Fig. 4 from the same source shows the relationship to shock propagation of the mass coordinate for the sonic point just after the last good homology. The pressure waves reaching the edge of the homologous core at this time must generate a shock at the sonic point.

The shock is more likely to stall if it has to traverse more mass during its passage outwards.

TABLE 1: The Effect of Equation of State on Shock Parameters for Two Models

Initial Model	$K_0(1/3)$	$\gamma$	$R_{\max}$ (km)	$\rho_{\max}^c$ ( $g/cm^3$ ) <sup>1/4</sup>	$E_S$ (foes)
(BCK) I (a) 0.6	220	2	300	4.67	0.30
(b) "	150	2	835	5.54	0.64
(c) "	120	2	(1200)	6.08	0.96
(WWF) II (a) 0.67	220	2	160	4.80	1.47
(b) 0.67	120	2	320	5.60	1.80

Model I is artificially constructed with core mass  $M_{\text{core}} = 1.32 M_{\odot}$ ; Model II is that of WWF [13].  $R_{\max}$  is the largest radius reached by the shock before stalling. In I(c) the shock is marginally successful in ejecting the mantle.  $\rho_{\max}$ , the maximum central density reached during collapse, is to be compared with  $\rho_0[(Z/A) = .32] = 2.3 \times 10^{14} \text{ gm/cm}^3$ . The energy  $E_S$ , a measure of shock energy discussed in BCK [15], is evaluated when the shock is at the lagrangian coordinate  $M = 1.21 M_{\odot}$ .

We concluded from our studies of the EOS in a Newtonian setting that indeed shock energies are enhanced. We mapped out the losses per unit mass traversed by the shock, but were forced to accept the unlikelihood of a prompt explosion in the realistic evolutionary models. One interesting point, however, was the rapid increase in central density associated with the softening of higher density nuclear matter.

#### IV. HYDRODYNAMIC SIMULATION: GENERAL RELATIVISTIC GRAVITATION

The Schwarzschild radius of some 2 km for a homologous core of  $0.7 M_{\odot}$ , which collapses to 15-20 km in radius, coupled to the cancellation of core internal and gravitational energies, alluded to above, suggests that the effects of general relativity cannot be ignored. The softer EOS further motivates the introduction of relativity, since non-linear gravitational effects are larger for the increased central densities. At first sight the strengthening of gravity inherent in general relativity will lead to deeper digging into the gravitational potential. However, this strengthening may also produce a smaller homologous core, and hence force the shock to traverse more matter on its way out. Indeed, early work by VAN RIPER [25] and TAKAHARA and SATO [26] suggested general relativity might be harmful to shock health, but VAN RIPER noted the possible sensitivity to the EOS. It is the unique combination of the softer EOS and relativistic gravitation present in our calculations that changes the picture.

The Newtonian force equation (12) is replaced by (see MISNER and SHARP [27])

$$\Delta_t U = e^{-\phi} \frac{\partial U}{\partial t} = - \frac{4\pi GR\rho}{c^2} - \frac{Gm}{R^2} - \frac{4\pi R^2}{\omega} \frac{\partial P}{\partial m} \quad (13)$$

with a gravitational mass

$$\tilde{m}(m,t) = \int_0^{R(m)} 4\pi R^2 \rho(1 + E/c^2) dR, \quad (14)$$

and where  $m$  is a comoving Lagrangian coordinate in terms of which the metric is

$$ds^2 = g_{\mu\nu} dx^\mu dx^\nu = - e^{2\phi} c^2 dt^2 + e^{2\lambda} dm^2 + R^2 d\Omega^2. \quad (15)$$

The factor  $\bar{\Gamma}$  in (13) is related to the radial metric coefficient by  $e^{2\lambda} = \left(\frac{\partial R}{\partial m}\right)^2 \bar{\Gamma}^{-2}$ , while the specific enthalpy is  $w = 1 + E/c^2 + \frac{P}{\rho c^2}$ .

The metric must be matched to an exterior Schwarzschild solution at some low-density surface  $m = m_g(t)$ , thus introducing the total mass-energy within this surface. The stress energy tensor is taken to be that of a perfect fluid. Eq. (13) must be solved using the EOS for the pressure together with the comoving energy equation

$$\frac{dE}{dt} = -\frac{d(1/\rho)}{dt} - e^{\phi} \dot{s} \quad (16)$$

Here  $\dot{s}$  is the rate of energy loss in escaping neutrinos and  $e^{\phi}$  a (small) neutrino redshift.

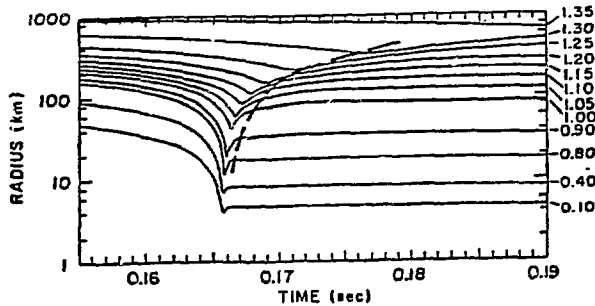


Fig. 5. The radius as a function of time for a collapsing general relativistic model. ( $12 M_{\odot}$  with  $\gamma = 3$ ,  $K_0(1/3) = 140$  MeV). The numbers on the right hand side indicate the total enclosed mass in units of  $M_{\odot}$ . The dotted line denotes the approximate position of the shock.

## V. RESULTS

Our general relativistic calculations have been performed using the initial models of WEAVER and WOOSLEY [2], with dramatic results. I have already referred to these latest models in the introduction, but note here they resemble WWF [13] in structure for  $M < 15 M_{\odot}$ , having iron cores with masses near  $1.36 M_{\odot}$ . However, between  $M = 15 M_{\odot}$  and  $20 M_{\odot}$ , a sudden change in core mass appears in the WW [2] analysis, a jump to core masses  $\geq 2.0 M_{\odot}$ . This discontinuity results from faster rates used for  $^{12}\text{C}(\alpha, \gamma)^{16}\text{O}$  (ROLFS [28]) and depends on the formation or non-formation of a carbon-burning shell. If the carbon-shell forms, its large entropy creates a barrier to further burning ending in iron. This is the case for the lighter initial stellar masses. Table 2 is a summary of numerical experiments carried out for several initial models differing in their parametrization of the EOS. Figure 5 contains the radius vs time profiles for the  $12 M_{\odot}$ , model 41 of Table 2. Reasonable choices for  $K_0(1/2)$ , very close if not within the range obtained by BLAIZOT [17], and for  $\gamma$  values near those expected from purely theoretical considerations, result in viable prompt explosions with energies adequate to account for any visual display. I wish to reemphasize that most of the softening from the near 200 MeV value of  $K_0(1/2)$  comes from the well understood extrapolation to asymmetric matter. Although one continues to characterize the nuclear EOS with  $K_0(1/2)$  it is the value near  $Z/A = 1/3$  that is most important for supernova calculations and not the history between  $Z/A = 1/2$  and  $1/3$ .

Table 2 Description of Calculations

Model	Mass ( $M_{\odot}$ )	$K_0^{sym}$ (MeV)	$K_0(0.33)$ (MeV)	$\gamma$	GR	$\frac{\rho_c^{max}}{\rho_0(0.33)}$	$E_{exp}$ (foes)	$E_{lost}$ (foes)
32	12	220	220	2	no	1.7	-	2.6
33	12	220	170	2	no	2.0	-	2.1
38	12	180	140	2	no	2.3	0.1	3.2
40	12	180	140	2	yes	12.0	3.2	2.2
41	12	180	140	3	yes	3.1	0.8	3.3
29	15	220	220	2	no	1.7	-	2.1
42	15	180	140	3	yes	3.1	-	2.5
43	15	180	140	2.5	yes	4.1	1.7	3.4
44	15	140	120	3	yes	3.3	-	3.2
45	15	90	90	3	yes	4.0	0.8	3.2

The column labeled GR refers to whether general relativity or Newtonian gravity was assumed.  $K_0(0.33)$  refers to the value of the nuclear incompressibility at saturation density when there are twice as many neutrons as protons ( $Z/A = 0.33$ ). For model 33 the form of the incompressibility was taken to be that of (3) with  $K_0^{sym} = 220$  MeV, while for models 38 and 40-43  $K_0^{sym}$  was chosen to be 180 MeV. Model 44 had  $K_0(x) = 140(1 - 1.3(1 - 2x)^2)$  and the other models (29, 32, 45) had  $K_0 =$  constant at the value given in this table.  $\gamma$  refers to the high-density adiabatic index discussed in the text.  $\rho_c^{max}$  is the maximum central density achieved just prior to bounce.  $E_{exp}$  is an estimate of the explosion energy, neglecting the binding energy of the mantle and envelope. No entry in this column means the shock failed to reach the edge of the iron core.  $E_{lost}$  is the total neutrino loss when the calculation was stopped (roughly 50 milliseconds after bounce).

"Successful" explosions in these calculations are most succinctly characterized by the maximum central density achieved during collapse (see Table 2). This may well be misleading, since phase changes to quark-gluon or other exotic forms of matter are excluded in our work, e.g. at sufficiently high density one expects hadron matter to coexist with two-flavour quark matter. Nevertheless, a high central density signals that the unfavourable aspects of general relativity, viz. the smaller homologous core and the perhaps stronger gravitational force the outward-moving shock must fight against, have been offset by an increase in the energy transferred to the shock from the gravitational well. An unexpected, but important, further advantage of stronger gravitation is occasioned by the faster collapse of the central core. The shock forms faster and will thus meet the infalling outer core zones at times when the latter are at lower density and falling slower. The passage outward is thus eased considerably relative to that of the Newtonian shock. This effect is illustrated in the density profiles in Fig. 6.

To summarize the results: In Table 2 for the reasonable choices  $\gamma = 2.5$  and  $K_0(0.33) = 140$ , corresponding to  $K_0(1/2) = 180$  MeV, one finds explosion energies near 2.0 foes in the general relativistic calculations. Lower shock energies are indeed acceptable, and one could probably produce prompt explosions for the 12  $M_{\odot}$  and 15  $M_{\odot}$  WW [2] models with  $K_0(0.50) = 200$  MeV, i.e. very close to the BLAIZOT [17] central value. These shock energies are not to be taken too seriously at this point, partly because of the uncertainties in our parametrizations and partly because the calculations should be followed further in time. Nevertheless, sufficient energy has been generated to eject the non-core regions of the star and to account for the visual display of a supernovae. Equally certain is that the remnant of such an explosion will be a neutron star, although its actual observable mass remains in some doubt.

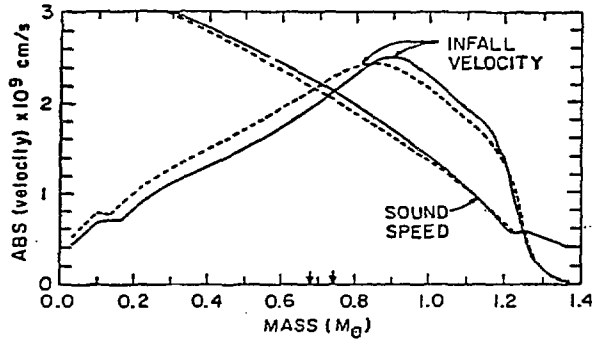


Fig. 6. Density profiles near bounce. In this case general relativity (dashed line) clearly produces a more favourable configuration for shock propagation.

#### VI. NEUTRON STAR MASSES

A possible constraint on the  $K_0, \gamma$  used in the nuclear EOS may result from a study of the hydrostatics of neutron stars. Inordinately soft matter would be unable to sustain the  $1.4 M_\odot$  mass observed for known neutron stars. For example, dropping the constant term in (1) yields as an appropriate non-saturating EOS for neutron matter:

$$P = \frac{K_0 \rho_0}{9\gamma} u^\gamma, \quad (16)$$

From calculations based on (16) one concludes  $\gamma \geq 2.5$  is required, a not very severe constraint in light of Table 2. However, one could easily imagine a density variation in the adiabatic index which kept  $\gamma$  low in the regions important in collapse while having  $\gamma$  rise sufficiently for  $\rho \geq 3$  to accommodate known neutron star masses. Such a choice would also go a long way towards explaining the Berkeley heavy ion experiments mentioned earlier. More work on the EOS is required for both the collapse and neutron star phases, and certainly more fundamental theoretical work incorporating amongst other things, the nuances of phase changes.

#### VII. CONCLUSIONS

In conclusion, we note, no Newtonian calculation with WW initial models yields sufficient energy to disrupt the star. The most favourable case for  $K_0(.33) = 140$  MeV and  $\gamma = 2$  (model 38) yields a shock which propagates off the mathematical grid, but whose .1 foe energy cannot overcome the few tenths of a foe binding of the mantle and envelope. There is a threshold of softness in nuclear matter beyond which the effects of general relativity become helpful to shocks. Shock energies are enhanced over Newtonian values by an order of magnitude reasonably close to this threshold in  $K_0(.33)$  and  $\gamma$ .

The WW initial models [2] for stars more massive than, perhaps,  $18 M_\odot$ , possessing iron cores greater than  $2.0 M_\odot$  in mass, will not explode; there is almost no chance for a hydrodynamic shock to be viable in such a massive core. Perhaps the delayed neutrino-heating scenario of Wilson and collaborators [29] is then appropriate. However, the use by nature of more than one means of producing type II supernova appears inelegant. Arnett [30] has put forward yet another mechanism for reviving stalled shocks: convection generated by the gradients in  $Y_e$  and entropy behind the shock. Baron, Bethe, Brown, and Cooperstein [31] have examined this possibility for the model 42 of BCK (Table 2) and conclude that although convection is indeed possible sufficiently far behind the shock, the details of the matter and energy distribution render such convection unfavourable to further progress of the shock.

Undoubtedly we have not yet heard the end of this tale, although I believe an important watershed has been reached. Initial models still retain the capacity for terror, for example a drop in core masses below  $1.25 M_\odot$  would dissolve all diffi-

culries, while an appreciable increase in core mass would prevent any prompt shock from succeeding. Finally, the details of nucleosynthesis must be followed hydrodynamically for a successful shock-produced explosion, and thus the initial stellar mass range required to partake in supernova for an adequate description of the known elemental abundances, would be defined.

## REFERENCES

1. E. Baron, J. Cooperstein, and S.H. Kahana: Phys. Rev. Lett. 55, 126 (1985).
2. S. E. Woosley and T.A. Weaver: Bull. Am. Astr. Soc. 16 971 (1984).
3. E.M. Burbidge, G.R. Burbidge, W.A. Fowler, and F. Hoyle: Rev. Mod. Phys. 29 547 (1957).
4. S.A. Colgate and H.J. Johnson: Phys. Rev. Lett. 5 235 (1960).  
S.A. Colgate and R.H. White: Ap. J. 142 626 (1966).
5. T.J. Mazurek, J. Cooperstein, and S.H. Kahana: DUMAND '80, ed. V.J. Stenger (DUMAND Center, Honolulu, 1981).  
T.J. Mazurek, J. Cooperstein, and S.H. Kahana: Supernovae: a Survey of Current Research, ed. M. Rees and R.J. Stoneham (Reidel, Dordrecht, 1982).
6. J.R. Wilson: Ann. N.Y. Acad. Sci. 336 358 (1980).
7. W.D. Arnett: Supernovae: a Survey of Current Research, ed. M. Rees and R.J. Stoneham (Reidel, Dordrecht, 1982).
8. W. Hillebrandt: Supernovae: a Survey of Current Research, ed. M. Rees and R.J. Stoneham (Reidel, Dordrecht, 1982).
9. J. Cooperstein: PhD thesis, State University of New York at Stony Brook (unpublished).
10. J. Cooperstein, H.A. Bethe, and G. E. Brown: Nucl. Phys. A429 527 (1984).
11. S.H. Kahana, E. Baron, and J. Cooperstein: in Problems of Collapse and Numerical Relativity, ed. D. Bancel and M. Signore (Reidel, Dordrecht, 1984) p. 163.
12. T.A. Weaver, B. Zimmerman, and S.E. Woosley: Ap. J. 225 1021 (1978).
13. T.A. Weaver, S.E. Woosley, and G.M. Fuller: Bull. Am. Astr. Soc. 14 No.4 957 (1982) and in Numerical Astrophysics, ed. J. Centrella, J. Leblanc, and R. Bowers (Jones and Bartlett, Boston, 1982).
14. H.A. Bethe, G.E. Brown, J. Applegate, and J. Lattimer: Nucl. Phys. A324 487 (1979).
15. E. Baron, J. Cooperstein, and S.H. Kahana: Nucl. Phys. A440 744 (1985).
16. J-P. Blaizot: Phys. Rep. 64 171 (1980).
17. K. Kolehmainen, M. Prakash, J. Lattimer, and J. Treiner: Nucl. Phys. A (to be published).
18. J.W. Harris, R. Bock, R. Brockmann, A. Sandoval, R. Stock, H. Stroebel, G. Odyniec, H.G. Pugh, L.S. Schroeder, R.E. Renfordt, D. Schall, D. Bangert, W. Rauch, and K. Wolf: Phys. Lett. 153 377 (1982).
19. R. Stock, R. Bock, R. Brockman, J.W. Harris, A. Sandoval, H. Stroebale, K.W. Wolf, H.G. Pugh, L.S. Schroeder, M. Maier, R.E. Renfordt, A. Daga, and M.E. Ortiz: Phys. Rev. Lett. 49 1236 (1982).
20. H.A. Gustafsson, H.H. Gutbrod, B. Kolb, H. Löhner, B. Ludwigt, A.M. Poskanzer, T. Renner, H. Riedesel, H.G. Ritter, A. Warwick, F. Weik, and H. Wieman: Phys. Rev. Lett. 52 1590 (1984).
21. Y. Kitazoe, M. Gyulassy, P. Danielewicz, H. Toki, Y. Yamamura, and M. Sano: Phys. Lett. 138B 341 (1984).
22. E. Baron, G.E. Brown, J. Cooperstein, and M. Prakash: SUNY at Stony Brook, preprint.
23. J.J. Molitoris and H. Stöcker: Phys. Rev. C32 346 (1985).
24. R. Epstein and C.J. Pethick: Ap. J. 243 1003 (1981).
25. K. Van Riper: Ap. J. 232 558 (1979).
26. M. Takahara, and K. Sato: Prog. Theor. Phys. 72 978 (1984).
27. C. Misner and D. Sharp: Phys. Rev. 136 571 (1964).
28. C. Rolfs: See for example the proceedings of the April 1986 Erice symposium on Nuclear Physics.
29. J.R. Wilson: in Numerical Astrophysics, ed. J. Centrella, J. Leblanc, and R. Bowers (Jones and Bartlett, Boston, 1985).
30. W.D. Arnett: to be published, (1985).
31. E. Baron, H.A. Bethe, G.E. Brown, and J. Cooperstein: Private communication (1986).